Quantum cluster equilibrium theory of liquids part I: Molecular clusters and thermodynamics of liquid ammonia

ARTICLE *in* BERICHTE DER BUNSENGESELLSCHAFT/PHYSICAL CHEMISTRY CHEMICAL PHYSICS · FEBRUARY 1998

DOI: 10.1002/bbpc.19981020210

3 AUTHORS, INCLUDING:

Ralf Ludwig
University of Rostock
275 PUBLICATIONS **5,139** CITATIONS
SEE PROFILE

Frank Weinhold
University of Wisconsin–Madison
199 PUBLICATIONS **28,776** CITATIONS
SEE PROFILE

Quantum Cluster Equilibrium Theory of Liquids Part I: Molecular Clusters and Thermodynamics of Liquid Ammonia

R. Ludwig *)

Physikalische Chemie, Fachbereich der Universität Dortmund, D-44221 Dortmund, Germany

F. Weinhold and T.C. Farrar

Theoretical Chemistry Institute and Department of Chemistry, University of Wisconsin-Madison, Madison, Wisconsin 53706, USA

Key Words: Clusters / Liquids Molecular Structure / Quantum Mechanics / Thermodynamics

The quantum cluster equilibrium (QCE) theory is presented for liquid ammonia. The cluster equilibria that dictate phase composition are determined by the rigorous techniques of quantum statistical thermodynamics in the canonical ensemble, based on the ab initio partition function. The characteristic features of the supra-molecular clusters which comprise the QCE model are discussed in terms of binding energies, geometries, cooperativity and charge transfer. Many possible equilibrium structures of ammonia are strongly disfavored for enthalpic and/or entropic reasons and do not show up in the QCE cluster populations. The numerical accuracy of the resulting QCE model is demonstrated by comparison with experimental data for thermodynamic properties of ammonia such as Clausius-Clapeyron pressure dependence and specific heat.

1. Introduction

Recently [1–5] clusters ("van der Waals molecules") which are found to be the fundamental micro structural building blocks of fluids, and whose properties can be determined by modern ab initio quantum mechanics and statistical thermodynamics. Standard quantum statistical thermodynamic methods are used to treat the equilibria between clusters in the canonical ensemble, leading to fully quantal predictions of macroscopic thermodynamic behavior. The QCE treatment relies on the close analogies between the covalent interactions of ordinary chemical equilibria and the noncovalent interactions of cluster equlibria, particularly those involving hydrogen bonding.

We present here the first application of the QCE formalism to liquid ammonia. Ammonia is chosen because it represents a relatively simple H-bonded fluid, for which a particularly wide range of calculated thermodynamic and spectroscopic properties can be compared with experimental data. A specific goal of the present work is to elucidate (through analysis of the wavefunctions; see below) the importance of non-pairwise-additive cooperative interactions for condensation phenomena. Since the QCE approach makes direct use of the ab initio cluster energetics, it is unnecessary to approximate liquid interactions with empirical potential functions of pairwise-additive form such as those commonly used in molecular dynamics simulations and Monte Carlo studies.

In the first paper we describe the ab initio calculations for supra molecular clusters of ammonia used throughout this work. We specifically focus on the strenght of hydrogen bonding, charge transfer and cooperative effects and their influence on bond lengths and bond angles. The results of the QCE model are then applied to thermodynamic properties of liquid ammonia. In a forthcoming paper, hydrogen bonding sensitive spectral probes such as vibrational frequencies, chemical shifts and quadrupole coupling constants are discussed for ammonia clusters. Using the QCE theory these NMR and infrared parameters are calculated as a function of temperature and are compared with spectroscopic data from NMR, Raman and IR measurements. Comparison of these theoretical values with experimental data provides a stringent test of the QCE population distributions and the associated (T, P)-dependent cluster picture of equilibrium liquid structure.

2. Theoretical Methods

2.1 Wave Function Calculation and Counterpoise Corrections

Ab initio supra molecular calculations were carried out at the uncorrelated restricted Hartree-Fock (RHF) level for a large number of ammonia clusters which are shown in Figs. 1 and 2. The calculations were carried out at the 3-21 G basis level for all molecular clusters and, additionally, at the 6-31+G* basis level for those ammonia clusters which according to the QCE formalism, are the predominate species present in the liquid phase. The 6-31+G* basis level augments the standard double zeta plus polarization treatment (6-31G*) with a diffuse set of s,p functions (+) on each heavy atom. Although ab initio supra molecular calculations have been highly successful in describing the structure and spectroscopy of hydrogen bonded species [6], they are known to be susceptible to artifacts of basis set super position error (BSSE) in finite basis sets. The most commonly accepted way to correct for BSSE is with counterpoise (CP) corrections [8], which we have applied to all calculations in the present work, even though the 6-31+G* basis set is known to markedly reduce BSSE. Harmonic vibrational frequencies were computed for the minimum energy structures and scaled by the standard factor 0.89 to correct for known systematic errors of the Hartree-Fock approximation. Calculations

*) Author to whom correspondence should be addressed.

  0005-9021/98/0202-0197 $ 17.50+.50/0

on an improved level of theory (MP2) and a larger basis set (6-311G(2f,p)) for the ammonia dimer yield better frequencies but still require a scaling factor of about 0.95.

2.2 Natural Bond Orbital Analysis

For the ammonia clusters which were calculated at the RHF/6-31+G* level of theory, the counterpoise-corrected binding energies were calculated and the wave functions were analyzed by the natural bond orbital (NBO) method [7], a standard program option of Gaussian 94. NBO analysis transforms the delocalized many-electron wave functions into optimized electron pair bonding units, corresponding to the Lewis structure picture. Starting from a given input atomic orbital basis set, the program performs a transformation to form a set of high-occupancy Lewis-type (bond, lone pair) NBO's, each of which is taken to be doubly occupied. This is said to represent the "natural Lewis structure" of the molecule. Delocalized effects, which appear as weak departures from the idealized localized picture, appear as nonzero occupancies of non-Lewis (anti-bond, Rydberg) NBO's. The total non-Lewis occupancy (ρ_{NL}) constitutes a quantitative measure of electronic delocalization. The results of NBO analysis allow many of the quantitative trends in cluster structure, stability, and spectroscopic properties to be rationalized in terms of non-pairwise-additive charge transfer delocalization between monomers.

2.3 The QCE Model

To calculate the cluster populations we used ab initio optimized geometries, harmonic frequencies, and binding energies. These values were than used to calculate an ab initio partition function for each cluster using standard statistical thermodynamic methods. In the electronic partition function ab initio RHF/3-21G binding energies are corrected with full counterpoise calculations [8] for the effects of basis set superposition errors. Residual cluster-cluster interactions are taken into accont by a mean-field correction which is proportional to the system density [1].

Some limitations of the present QCE model should be noted. Although qualitatively reasonable, the mean-field treatment is not entirely satisfactory. The mean-field coefficient "c_{mf}" is an "empirical" parameter representing effects not explicitly included in the ab initio clusters. In principle, interactions of the clusters with the surrounding medium might be estimated from average multipole and dispersion properties of the cluster distribution, or by self-consistent reaction field techniques. But in initial applications we simply choose "c_{mf}" to fix a specific thermodynamic property at single T, P. However, even complete neglect of this correction does not grossly affect equilibrium liquid populations and has practically no effect on gas-phase properties. The current treatment of molecular volume used in evaluating the translational partition function is also a limiting factor. However, an overall proportionality factor "b_{vdw}" (chosen to fix system density at a single point, e.g. standard state) can be altered to verify that gross populations are relatively insensitive to these volume estimates. A further limitation of the current work is the use of the harmonic approximation in the evaluation of the vibrational partition function, but the consequences of this rather unsatisfactory treatment (particularly, of low-frequency vibrations) is rather difficult to assess at the current level of ab initio technology. The results for the cluster populations clearly depend on whether all significant clusters have been included in the molecular system, and this has been tested by exploring a much wider range of clusters at the 3-21G level than was found necessary to include in the final 6-31+G* cluster mixture.

As remarked in the Introduction, the conditions of chemical equilibrium are employed to find the cluster populations for the phase of lowest free energy at a specific temperature and pressure. In the present case, for example, the stable liquid phase at standard-state conditions is calculated to lie 4.22 kJ/mol below the low density vapor phase.

3. Results and Discussion

3.1 Cluster Structural and Energetic Properties

3.1.1 Binding Energies

Figs. 1 and 2 show all significant ammonia cluster species generated at the RHF/3-21G level for incorporation in the QCE model: ammonia monomer (NH_3) linear dimer $(NH_3)_{2l}$, cyclic trimer $(NH_3)_{3c}$, tetramer $(NH_3)_{4c}$, and pentamer $(NH_3)_{5c}$, as well as various "star-like" topologies with one or two monomers appended to a cyclic framework (e.g. $(NH_3)_{4c+1}$ having an exocyclic monomer attached to a cyclic tetramer). As shown later, the species in Fig. 2 do not contribute significantly to the RHF/3-21G QCE cluster populations because of enthalpic and/or entropic reasons and were omitted in the final RFH/6-31+G* cluster mixture.

Except for the monomer, NH_3, and the dimer $(NH_3)_{2l}$, the clusters included in the QCE model are based on bi-coordinatively linked ring structures which previous studies have shown to have favorable thermodynamic stability in the liquid region. In such structures each monomer participates in a matched pair of H-bonds, once as a Lewis base (electron-pair "donor") and once as a Lewis acid (electron pair "acceptor"). As described in previous studies of H-bond cooperativity [17, 18], such bi-coordinate structures allow inter molecular electron delocalization ("charge transfer") to occur in a maximally concerted manner, leading to strong non-pairwise-additive enhancements of binding energies. For those ammonia structures in which all monomers participate as "donor" and "acceptor" as well, the cooperative effects lead to H-bonding energies that are significantly stronger than the linear dimer hydrogen bond energy.

The effectiveness of such topologies in increasing average H-bond strength is indicated in Table 1 where we pre-

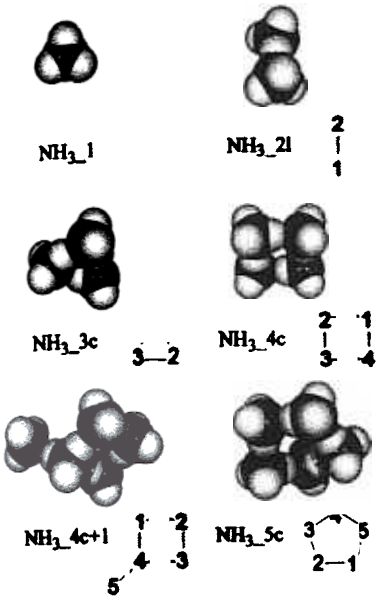

Fig. 1
The most significant equilibrium ammonia clusters as predicted by the QCE model: ammonia monomer $(NH_3)_1$, linear dimer $(NH_3)_{2l}$, cyclic trimer $(NH_3)_{3c}$, cyclic tetramer $(NH_3)_{4c}$, mixed pentamer $(NH_3)_{4c+1}$ and cyclic pentamer $(NH_3)_{5c}$

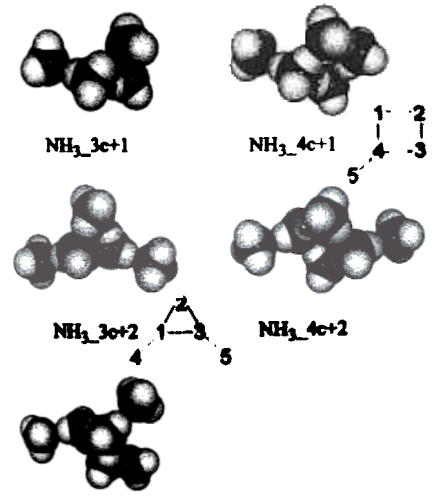

Fig. 2
Equilibrium ammonia clusters ruled out by the QCE model: mixed cyclic and star-like structures: tetramer $(NH_3)_{3c+1}$, pentamer $(NH_3)_{3c+2}$ and $(NH_3)_{4c+1}$, and hexamers $(NH_3)_{3c+3}$, $(NH_3)_{4c+2}$

sent the calculated RHF/6-31+G* Hartree-Fock energy, the CP-corrected total energy (E_{CP}), the average binding energy per H-bond ($\Delta\bar{E}_{HB}$) and percentage cooperative enhancement (%-coop., with respect to H-bond strength in the ammonia dimer $(NH_3)2l$) for all clusters shown in Fig. 1. The cooperative energies cited here are "average" energies. The average energy of all cluster H-bonds increases significantly with cluster size (trimer 11%, tetramer 24% and pentamer 25%). Cooperative enhancement stabilizes the pentamer by about 12.01 kJ/mole, equivalent to adding more than one "new" H-bond beyond the sum of nominal (pairwise additive) dimer H-bonds. We

Table 1
Cooperative energetics of H-bonding in ammonia clusters showing the calculated RHF/6-31+G* Hartree-Fock energy (E_{RHF}, a.u.), counterpoise-corrected total energy (E_{CP}, a.u.), average H-bond energy ($\Delta\bar{E}_{HB}$, kJ/mol), and percentage cooperative enhancement (% coop., relative to dimer H-bond energy of 9.62 kJ/mol)

Species	E_{RHF} a.u.	E_{CP} a.u.	$\Delta\bar{E}_{HB}$ kJ/mol	% coop.
$(NH_3)_1$	-56.189499	-		
$(NH_3)_{2c}$	-112.383395	-112.382659	9.62	
$(NH_3)_{3c}$	-168.582439	-168.580641	10.63	11.05
$(NH_3)_{4c}$	-224.779848	-224.776222	11.96	24.43
$(NH_3)_{5c}$	-280.975269	-280.970365	12.01	24.82
$(NH_3)_{4c+1}$	-280.972293	-280.968008	10.77	11.20

can therefore judge that cooperative "corrections" increase the strength of particular hydrogen bonds, and these effects are close to saturation at the largest cluster sizes considered.

3.1.2 *Equilibrium Geometries*

Cooperative enhancement of binding energies also leads to significant geometry changes for the ammonia clusters. The optimized structures obtained with the 6-31+G* basis set at the Hartree-Fock-level appear to provide quite accurate geometries. Calculated values are shown in Table 2 along with a comparison of the experimentally determined geometries of isolated gas phase molecules obtained from electron diffraction studies [11, 12].

The calculated geometries for all molecules in the clusters and the average geometries for the clusters are given in Table 3. In Fig. 3 the variations of the NH bond length, r_{NH}, and the HNH bond angle, $<_{HNH}$, with cluster size are shown[1]. As a consequence of cooperative enhancement and increasing hydrogen bond strength with larger cluster size, r_{NH} increases by about 0.33 pm and $<_{HNH}$ decreases by about 0.6° going from the monomer up to the five membered cyclic cluster.

The observed trend for the N-H bond length and H-N-H bond angles is supported by the measured properties in solid and gaseous ammonia. Despite the experimental uncertainties it may be concluded that going from the gas to the solid phase the N-H bond lengths are increased and the bond angles are decreased [13]. The calculated values appear to be in reasonable accord with this rather uncertain experimental data.

It is interesting to note the variation of the inter molecular bond for the nitrogen atoms $r_{N\cdots N}$ shown in the Fig. 4. The dimer value of about 3.38 Å decreases down to 3.31 Å in the cyclic pentamer of ammonia. This consequence of cooperativity was recently demonstrated by Saykally et al. [14–16] who investigated experimentally

[1] Here, again we are referring to average bond lengths and angles. The bond lengths for the inner molecules change by a greater amount than those at the ends of the cluster.

Table 2
Intramolecular distances (in Å) and bond angles (in degrees) of the ammonia monomer from ab initio calculations on the 6-31+G* basis set and from electron diffraction studies

X	State	r_{NH}	$\langle_{HNH}$	Method	Reference
H	Monomer	1.002	108.1	ab initio	This work
H	Gas	1.019	109.1	ED	[11]
H	Gas	1.030	–	ED	[12]
D	Gas	1.020	106.1	ED	[11]
D	Gas	1.026	–	ED	[12]

the inter molecular distance $r_{O\cdots O}$ in different sized water clusters. As predicted by ab initio calculations the $r_{O\cdots O}$ distance decreases with increasing cluster sizes. A more detailed discussion of the geometries will be given in a subsequent paper.

3.1.3 *Cooperativity and Charge-Transfer*

As in previous NBO studies of $r_{A-H\cdots B}$ complexes [7], the ubiquitous role of $n_B \rightarrow \sigma^*_{AB}$ "donor-acceptor" interactions in hydrogen bonding is exhibited by ammonia clusters. The intermolecular delocalization from a "filled" lone pair n_B of the donor (Lewis base) B: into an adjacent "unfilled" antibond σ^*_{AH} of the acceptor (Lewis acid), A-H can qualitatively rationalize many of the factors that stabilize certain H-bond clusters relative to others.

We consider first the simple linear dimer, where the electron-pair donor is a nitrogen lone pair (n_N) and the electron-pair acceptor is an N-H anti bond (σ^*_{NH}) [17] as shown in Fig. 5. The general $n_N \rightarrow \sigma^*_{NH}$ interaction leads to an energetic stabilization that can be estimated from simple perturbation theoretical considerations [17] as

$$\Delta E^{(2)}_{n_N \rightarrow \sigma^*_{NH}} \cong -2\frac{\langle n_N|\hat{F}|\sigma^*_{NH}\rangle^2}{E_{\sigma^*_{NH}} - E_N} \quad (1)$$

This is an intermolecular analog of the familiar "2e-stabilization" effect [19]. Here $\langle n_N|\hat{F}|\sigma^*_{NH}\rangle$ is the Fock matrix element, approximately proportional to the PNBO overlap $S_{n_N-\sigma^*_{NH}}$ and $E_{\sigma^*_{NH}} - E_N$ is the orbital energy difference for the σ^*_{NH} and n_N NBOs, as shown in Fig. 5.

The stabilization energy is expected to be the principal attractive contribution to H-bond formation and is closely related to the cooperative strengthening and shortening of H-bonds, since intermolecular charge delocalization enhances the Lewis base (donor) strength of one monomer and the Lewis acid (acceptor) strength of the other. Table 4 presents the $\Delta E^{(2)}_{n_B \rightarrow \sigma^*_{NH}}$ delocalization energies for different $(NH_3)x$ clusters. It is seen that the strongest intermolecular stabilization $\Delta E^{(2)}_{n_B \rightarrow \sigma^*_{NH}}$ is found for the largest cyclic structures and is obviously related with the cooperative binding energies (Table 1) and geometry changes (Table 3).

Table 3
Ab initio bond length (in Å) and bond angles (in °) calculated for different molecular clusters of ammonia. The superscripts f and b indicate whether corresponding atoms are free or H-bonded

Geometry	$(NH_3)_1$	$(NH_3)_{2t}$	$(NH_3)_{3c}$	$(NH_3)_{4c}$	$(NH_3)_{5c}$	$(NH_3)_{4+1}$
r^b_{NH}		1.0046	1.0078	1.0078	1.0079	1.0090
			1.0078	1.0078	1.0079	1.0053
				1.0078	1.0078	1.0080
				1.0078	1.0080	1.0074
					1.0079	1.0080
r^f_{NH}	1.0020	1.0024	1.0029	1.0032	1.0032	1.0034
		1.0024	1.0029	1.0032	1.0033	1.0033
		1.0026	1.0029	1.0032	1.0033	1.0034
		1.0030	1.0029	1.0032	1.0034	1.0032
		1.0026	1.0029	1.0032	1.0034	1.0031
			1.0029	1.0032	1.0033	1.0031
			1.0029	1.0032	1.0033	1.0032
				1.0032	1.0033	1.0032
				1.0032	1.0033	1.0026
					1.0033	1.0024
					1.0033	1.0026
aver.	1.0020	1.0032	1.0041	1.0047	1.0048	1.0045
$\langle^b_{HNH}$		108.177	107.932	107.574	107.361	107.463
		108.177	107.932	107.574	107.630	107.993
			107.932	107.574	107.397	107.616
			107.932	107.574	107.610	107.554
			107.932	107.574	107.380	107.568
			107.932	107.574	107.496	107.706
				107.574	107.383	107.338
				107.574	107.370	107.226
					107.313	107.226
					107.500	
$\langle^f_{HNH}$	108.125	107.674	107.298	107.083	107.139	106.993
		107.743	107.298	107.083	107.143	107.156
		107.787	107.298	107.083	107.059	107.089
		107.787		107.083	106.976	107.906
					107.017	107.888
						107.226
						107.822
	108.125	107.891	107.509	107.410	107.318	107.436
r_{NN}		3.3753	3.3130	3.3067	3.3009	3.2742
			3.3160	3.3068	3.3070	3.3838
				3.3065	3.3180	3.3230
				3.3065	3.3168	3.3027
					3.3046	3.4407
aver.		3.3753	3.3130	3.3066	3.3095	3.3450
$\langle_{N-HN}$	166.31	156.146	172.791	175.057	173.869	
			156.146	172.791	176.961	170.112
				172.791	179.341	173.837
				172.791	179.617	173.379
					176.845	171.521
aver.		166.31	156.146	172.791	177.564	172.544

As H-bond strength increases and $r_{N-H\cdots N}$ distances decrease, there is progressive charge transfer into the σ^*_{NH} antibond. The charge transfer (q_{CT}) can be estimated from standard perturbation-theoretic considerations as

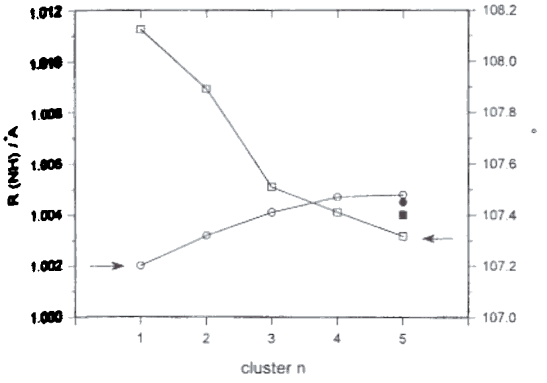

Fig. 3
Ab initio calculated bond lengths r_{NH} (circles) and bond angles $\langle_{H-N-H}$ (squares) in ammonia as a function of cluster size. The filled symbols are the calculated values for the $(NH_3)_{4c+1}$ pentamer

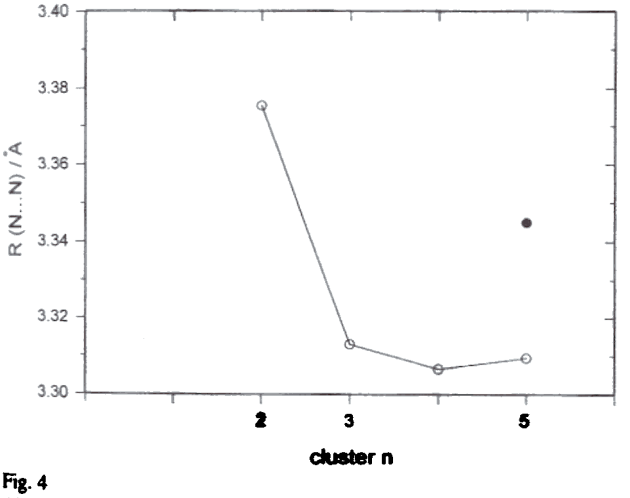

Fig. 4
Ab initio calculated intermolecular bond lengths $r_{(N\cdots N)}$ (squares) of ammonia clusters depending on the cluster size. The filled symbols are the calculated values for the $(NH_3)_{4c+1}$ pentamer

$$q_{CT} = 2|\lambda|^2 = 2\left\{ \right. \qquad \mathbf{2}$$

As shown in Table 5, favorable cooperative stabilization tends to be associated with a maximum number of "CT-neutralized" monomers, having an equal number of donor-acceptor interactions "in" and "out". The full cyclic structures have all monomers neutralized as "closed-CT" networks, which are indicate to have highest stability.

Three different pentamers $(NH_3)_{5c}$, $(NH_3)_{4c+1}$ and $(NH_3)_{3c+2}$ can be compared in this respect: in $(NH_3)_{5c}$, all monomers are close to CT-neutralized. In $(NH_3)_{4c+1}$ the monomers of the cycle have a small negative charge, but there is a strong positive charge on the added monomers which adversely affects stability. In $(NH_3)_{3c+2}$ the net charges of all are further increased, becoming more negative in the ring and more positive in the exocyclic monomer. Compared to the full cyclic structure, the more open-CT "star-like" topologies are therefore strongly disfa-

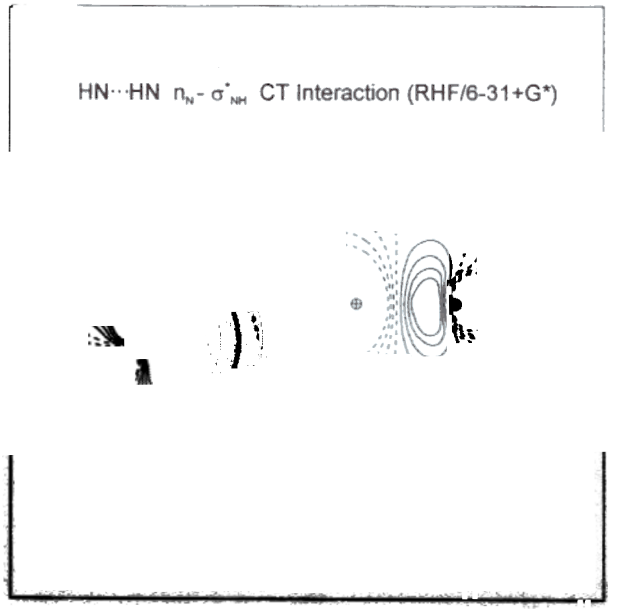

Fig. 5
Orbital contour diagram of overlapping nitrogen lone pair n_N and NH antibond (σ^*_{NH}) PNBOs in equilibrium $(NH_3)_{2l}$ dimer (RHF/6-31+G* level)

Table 4
NBO delocalization energies (kcal/mol) for $(NH_3)_n$ clusters (RHF/6-31+G* level), showing the 2nd-order perturbation estimate of the $n_N \rightarrow \sigma^*_{NH}$ delocalization energer $E^{(2)}_{n\rightarrow\sigma^*}$ from monomer k to monomer $k+1$

Species	$\Delta E^{(2)}_{1\rightarrow2}$				
$(NH_3)_{2l}$	5.36				
Species	$\Delta E^{(2)}_{1\rightarrow2}$	$\Delta E^{(2)}_{2\rightarrow3}$	$\Delta E^{(2)}_{3\rightarrow1}$		
$(NH_3)_{3c}$	5.55	5.55	5.55		
Species	$\Delta E^{(2)}_{1\rightarrow2}$	$\Delta E^{(2)}_{2\rightarrow3}$	$\Delta E^{(2)}_{3\rightarrow4}$	$\Delta E^{(2)}_{4\rightarrow1}$	
$(NH_3)_{4c}$	8.08	8.07	8.08	8.08	
Species	$\Delta E^{(2)}_{1\rightarrow2}$	$\Delta E^{(2)}_{2\rightarrow3}$	$\Delta E^{(2)}_{3\rightarrow4}$	$\Delta E^{(2)}_{4\rightarrow5}$	$\Delta E^{(2)}_{5\rightarrow1}$
$(NH_3)_{5c}$	8.37	8.39	8.45	8.32	8.28
Species	$\Delta E^{(2)}_{1\rightarrow2}$	$\Delta E^{(2)}_{2\rightarrow3}$	$\Delta E^{(2)}_{3\rightarrow4}$	$\Delta E^{(2)}_{4\rightarrow1}$	$\Delta E^{(2)}_{5\rightarrow4}$
$(NH_3)_{4c+1}$	8.17	7.64	6.15	9.33	5.02
Species	$\Delta E^{(2)}_{1\rightarrow2}$	$\Delta E^{(2)}_{2\rightarrow3}$	$\Delta E^{(2)}_{3\rightarrow1}$	$\Delta E^{(2)}_{4\rightarrow1}$	$\Delta E^{(2)}_{5\rightarrow2}$
$(NH_3)_{3c+2}$	3.79	6.81	4.90	4.81	4.96

Table 5
Calculated natural charges of each ammonia monomer in different clusters at RHF/6-31+G* levels of theory

Species	Unit	Unit 2	Unit 3	Unit 4	Unit 5
$(NH_3)_{2l}$	+0.00625	−0.00625	–	–	–
$(NH_3)_{3c}$	0.00000	0.00000	0.00000	–	–
$(NH_3)_{4c}$	0.00000	0.00000	0.00000	0.00000	–
$(NH_3)_{5c}$	0.00000	−0.00028	+0.00028	0.00000	0.00000
$(NH_3)_{4c+1}$	−0.00186	−0.00296	−0.00231	−0.00092	+0.00805
$(NH_3)_{3c+2}$	−0.00413	−0.00358	−0.00366	+0.00576	+0.00561

Table 6
Temperature dependent populations (in %) of the various ammonia clusters from thermodynamic calculations (RHF/3-21G)

T/K	(NH_3)	$(NH_3)_{2c}$	$(NH_3)_{3c}$	$(NH_3)_4$	$(NH_3)_5$	$(NH_3)_{4c+1}$
196	7.6		0.	7.7	82.1	1.3
200	8.6		0.	7.7	80.5	1.5
205	10.1	2.0		7.6	78.4	1.8
210		2.6	0.1	7.5		2.1
215	13.3	3.3	0.2	7.3	73.5	2.4
220	15.0	4.1	0.2	7.2	70.7	2.8
225	16.7	5.1	0.2	6.9	67.8	3.2
230	18.5	6.2		6.7	64.7	3.5
235	20.2	7.5		6.5	61.6	3.9
239		8.6		6.2	59.0	4.2

vored. As a consequence, for the QCE populations it is expected that pentamers structures appear in the order $(NH_3)_{5c} \geq (NH_3)_{4c+1} \geq (NH_3)_{3c+2}$, as is observed. This ordering reflects a general tendency that can be stated as follows: on enthalpic grounds, cooperative bicoordinated topologies are favored, with charge transfer "neutralized" at each monomer. Conversely, open-CT star topologies are strongly disfavored.

3.2 QCE Population Distributions and Thermodynamic Properties

The liquid phase cluster populations obtained from thermodynamic calculations for temperatures in the range of 196 (melting point) to 239 K (boiling point) are listed in Table 6 and shown in Fig. 6. Over the whole temperature range the cluster populations change significantly. At low temperatures the cyclic pentamers are the dominant species. At higher temperatures these clusters are partially replaced by dimers and monomers.

As discussed in Sect. 3.1, "closed-CT" networks such as the cyclic pentamer, (NH_{35c}), exhibit favorable electronic stability which allows them to survive in the QCE equilibrium population. Consequently, except for $(NH_3)_{4c+1}$, which appears in trace amounts and competes with $(NH_3)_{4c}$, mixed star-like structures do not show up in the QCE cluster population over any part of the liquid phase temperature range.

True cluster stability cannot be judged solely from the electronic energies, since one must also take into account entropic factors of vibtrational origin. A primary entropic factor is the presence of low-frequency "torsional" motions about the hydrogen bond, which are best preserved in bicoordinate chain or ring topologies. A second entropic effect is associated with bending and tilting vibrations in highly strained, non-linear H-bonds. These vibrations are of low frequency in the linear H-bond limit where the isotropic s-like "end" of the n_B, σ^*_{NH} orbitals are overlapping, leading to little energetic penalty for small deformations. Such strain-entropy effects are particularly evident in small cyclic structures. For example, on enthalpic grounds, the cyclic ammonia trimer has marginally higher

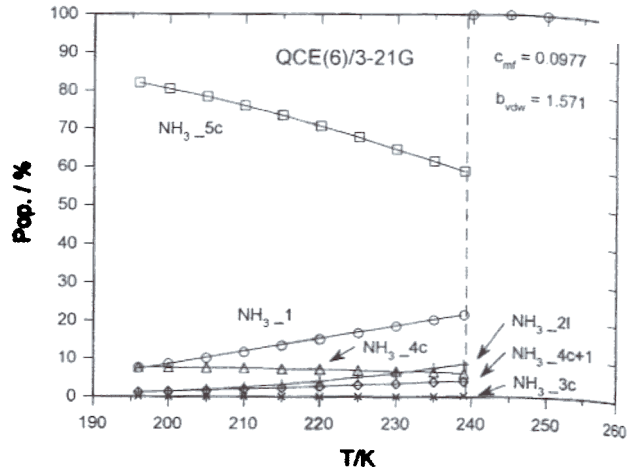

Fig. 6
Cluster populations for the QCE(6)/3-21G model of ammonia as a function of ammonia at $P = 1$ atm. As explained in the text, c_{mf} is a mean-field coefficient and b_{vdw} is a simple van-der-Waals-like correction factor that are used to fix, the boiling point and the density, at a single pressure

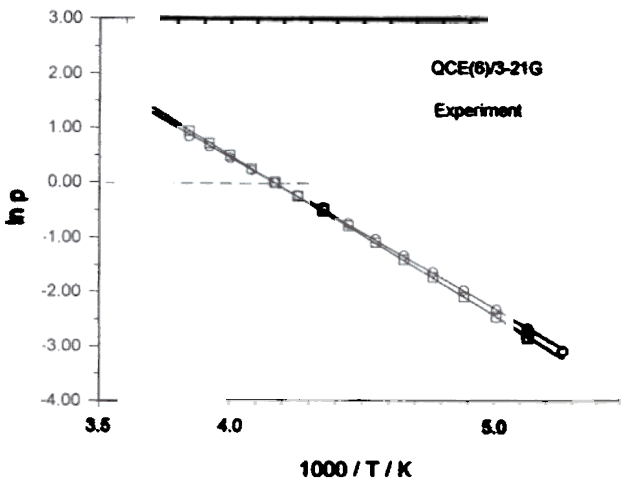

Fig. 7
Clausius-Clapeyron plot of ammonia vapor-pressure curve, comparing calculated QCE(6)/3-21G model (circles) with experimental values (squares). The slope of the QCE line at $P = 1$ atm corresponds to a standard enthalpy of vaporization of 23.2 kJ/mol, in excellent agreement with the experimental value, 23.8 kJ/mol [20, 21]

average H-bond strength than the dimer, and so might be expected to compete favorably with the dimer. However, the QCE trimer populations are always much smaller than those of dimers, which for enthalpic reasons are themselves disfavored compared to larger cyclic structures.

4. Comparisons of QCE Theory with Experiment

4.1 Thermodynamic Properties

The liquid phase cluster populations were obtained for points along the QCE/3-21G liquid-gas coexistence line. The pressure dependence of the theoretical vapor pressure

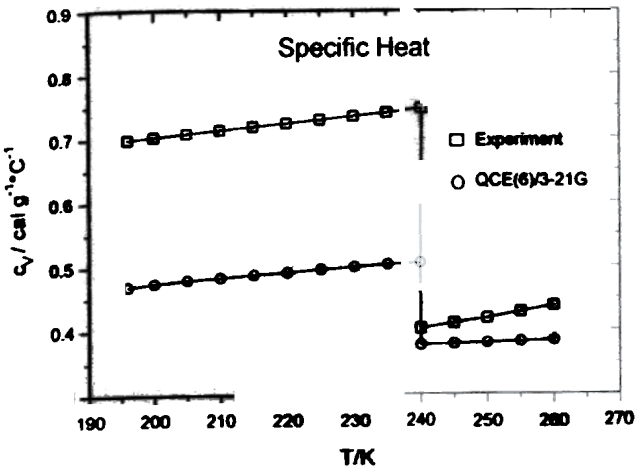

Fig. 8
Constant-volume specific heat c_v (cal/gC) of ammonia, comparing experimental (squares) with calculated QCE (6)/3-21G (circles) values. The experimental gas-phase c_p values from literature [20, 21] were converted to constant-volume c_v form with an ideal gas approximation

curve is shown in Fig. 7 as a Clausius-Clapeyron plot of $\log(P)$ vs. $1/T$. From the slope of this plot, the QCE standard enthalpy of vaporization is found to be 23.2 kJ/mol, in excellent agreement with the experimental value of 23.8 kJ/mol [20, 21].

Another important aspect of liquid phase behavior is the calorimetric response of internal energy E with respect to temperatures variations, quantified in terms of mole heat capacity, $C_v = \left(\frac{\partial E}{\partial T}\right)_v$, which samples the next higher temperature derivative of the partition function. Fig. 8 shows calculated QCE/3-21G values of specific heat and a comparison with experimental values in the region of the liquid/gas phase transition. As shown in the figure, the calculated values are qualitatively correct in the gas phase region, but in error in the liquid-phase region (about 30% too low). Here it should be pointed out that specific heats are quite sensitivie to the treatment of vibrational degrees of freedom (particularly, anharmonic corrections), and the present QCE model partition function does not adequately represent C_v (and other high-order T-derivatives).

5. Conclusions

The foregoing results provide a stringent and comprehensive experimental test of the ab initio QCE/3-21G model of liquid ammonia over the entire liquid range. Overall, one can conclude that the investigated thermodynamic properties with the QCE model are in reasonable qualitative agreement with the experimental findings. In view of the simplicity of the current QCE model, and the many possibilities for its improvement, the current agreement between theory and experiment is satisfactory.

The theoretical QCE model leaves many options for further improvement, including higher levels of basis level and correlation treatment, inclusion of vibrational anharmonicities and vibration-rotation coupling, more accurate evaluation of T-dependent excluded cluster volume, and improved treatment of intercluster interactions. The present QCE treatment employs two "empirial" parameters (the mean-field coefficient "c_{mf}" and excluded-volume correction factor "b_{vdw}") that have little influence on qualitative clustering patterns and can only be used to fix, e.g., the density and boiling point at a single pressure. Both should be superseded in a more satisfactory future version of the theory. Beside thermodynamic properties, the temperature dependent QCE behavior of hydrogen bonding sensitive probes such as chemical shifts, quadrupole coupling constants and vibrational frequencies presented in the following paper is of great help for that purpose.

R.L. thanks the Deutsche Forschungsgemeinschaft and the Fonds der Chemischen Industrie for financial support. We thank the National Science Foundation, grant number CHE-9500735 for the support of this research. We thank the referee for a number of helpful suggestions and comments.

References

[1] F. Weinhold, The nature of H-bonding in clusters, liquids and enzymes: an ab initio, natural bond orbital perspective, 1996.
[2] R. Ludwig, F. Weinhold, and T.C. Farrar, J. Chem. Phys. *103*, 6941 (1995).
[3] R. Ludwig, F. Weinhold, and T.C. Farrar, J. Chem. Phys. *102*, 5118 (1995).
[4] R. Ludwig, F. Weinhold, and T.C. Farrar, J. Chem. Phys. *103*, 3636 (1995).
[5] R. Ludwig, F. Weinhold, and T.C. Farrar, J. Chem. Phys. *107*, 499 (1997).
[6] P. Hobza and R. Zahradnik, Chem. Rev. *88*, 871 (1988).
[7] J.P. Foster and F. Weinhold, J. Am. Chem. Soc. *102*, 7211 (1980); A.E. Reed and F. Weinhold, J. Chem. Phys. *78*, 4066 (1983); E. Glendening, A.E. Reed, J.E. Carpenter, and F. Weinhold, NBO 4.0 Program Manual, Univ. of Wisconsin Theoretical Chemistry Institute Technical Report WISC-TCI-756, 1996.
[8] S.F. Boys and F. Bernardi, Mol. Phys. *19*, 553 (1970).
[9] For an authorative description of the ab initio methods and basis sets employed here, W.G. Hehre, L. Radom, P.v.R. Schleyer, and J.A. Pople, Ab initio molecular orbital theory, Wiley, New York, 1986.
[10] G94 Gaussian 94 (Revision A.1) A, M.J. Frisch, G.W. Trucks, H.B. Schlegel, P.M.W. Gill, B.G. Johnson, M.A. Robb, J.R. Cheeseman, T.A. Keith, G.A. Peterson, J.A. Montgomery, K. Raghavachari, M.A. Laham, V.G. Zakrzewski, J.V. Ortiz, J.B. Foresman, J. Cioslowski, B. Stefanov, A. Nanayakkara, M. Challacombe, C.Y. Peng, P.Y. Ayala, W. Chen, M.W. Wong, J.L. Andres, E.S. Replogle, R. Gomperts, R.L. Martin, D.J. Fox, J.S. Binkley, D.J. Defrees, J. Baker, J.J.P. Steward, M. Head-Gordon, C. Gonzalez, and J.A. Pople, Gaussian, Inc., Pittsburgh, PA, 1995.
[11] O. Bastiansen and B. Beagley, Acta Chem. Scand. *18*, 2077 (1964).
[12] K. Kuchittsu, J.P. Guillory, and L.S. Bartell, J. Chem. Phys. *49*, 2488 (1968).
[13] T. Brausewein, H. Bertagnolli, A. David, K. Goller, H. Zweier, K. Tönheide, and P. Chieux, J. Chem. Phys. *101*, 672 (1994).
[14] J.D. Cruzan, L.B. Braly, K. Liu, M.G. Brown, J.G. Loeser, and R.J. Saykally, Science *271*, 59 (1996).

[15] K. Liu, M.G. Brown, J.D. Cruzan, and R.J. Saykally, Science *271*, 62 (1996).
[16] K. Liu, J.D. Cruzan, and R.J. Saykally, Science *271*, 929 (1996).
[17] A.E. Reed, L.A. Curtiss, and F. Weinhold, Chem. Rev. *88*, 899 (1988).
[18] B.F. King and F. Weinhold, J. Chem. Phys. *103*, 333 (1995).
[19] I. Flemming, Frontier orbitals and organic chemical reactions, pp. 24–27, Wiley, New York, 1976.
[20] R. Overstreet and W.F. Giauque, J. Am. Chem. Soc. *59*, 254 (1937).
[21] L. Haar and J.S. Gallagher, J. Phys. Chem. Ref. Data *7*, 635 (1978).

(Received: August 26, 1997
final version: November 7, 1997) E 9691